Indian Journal of Chemistry
Vol. 64, March 2025, pp. 291-298
DOI: 10.56042/ijc.v64i3.16490

Antiproliferative activity of triterpenoids of *Nelumbo nucifera* Gaetrn. rhizomes and their derivatives: *In vitro* and *in silico* studies

Deepika Singh*[a], Shiv Kumar[b], Mahendra P Darokar[b] & Prabir K Chaudhuri[a]

[a] Medicinal Chemistry Division
and
[b] Molecular Bioprospection Department, CSIR-Central Institute of Medicinal and Aromatic Plants, PO CIMAP, Lucknow 226 015, India
E-mail: deepika.sh25@yahoo.com

Received 27 December 2024; accepted(revised) 27 February 2025

Breast cancer and prostate cancer are the most common malignancy in women and men, respectively. In view of serious side effects of the available therapies, cost of the treatment and drug-resistance, the search for more effective anticancer drug is urgently needed. Triterpenoids present inedible rhizomes of *Nelumbo nucifera* Gaetrn which possess antiproliferative activities. To investigate the therapeutic effect of *N. nucifera* triterpenoids against breast and prostate cancers, the semi-synthetic derivatives of triterpenoids have been prepared and monitored for their *in vitro* bioassay, molecular docking, QSAR and ADMET studies. Compound 2α, 3β, 24-triacetoxy hyptatic acid-A(**3c**) show significant inhibitory activity against breast cancer (MCF-7, IC_{50} = 9.77 ± 0.9 μM) along with the strong binding affinity towards the active site of 3ERT with docking score of –7.2 kcal/mol. The QSAR model suggests the importance of geometrical shape and dipole moment of triterpenoids for their antiproliferative activity against MCF-7 cells, while AlogP and DPSA_1 is crucial for showing the activity against PC-3 cells. The ADMET analysis demonstrates that the triterpenoids follow most of the physicochemical properties required for their optimum bioavailability and not showing any toxicity. In this study, hyptatic acid-A emerged as a good structural template to develop novel leads against different cancers and substitution at C24 hydroxyl group has important role in bioactivity.

Keywords: *Nelumbo nucifera* Gaertn., Triterpenoids, Antiproliferative activity, Estrogen receptor alpha, Androgen receptor

Cancer is a leading cause of death worldwide, accounting for nearly one in six deaths in year 2020[1]. Breast cancer (BC) is the leading cause of cancer deaths among women and nearly 75% of breast cancers demonstrate high expression of estrogen receptor (ER)[2]. Almost 74% of breast cancers are caused by the high expression of ER-alpha (ERα), therefore ERα remains a key therapeutic target for breast cancer[3]. The treatment of breast cancer with ER antagonists contributes to reduce the breast cancer mortality[4]. Prostate cancer (PC) is the second most prevalent among male[5].There were 1,467,854 new cases of PC reported in year 2022. Researchers found that AR is a potential and attractive target for PC therapy *via* AR antagonists or combined androgen blockade therapy for many years[6]. Several mechanisms underlying the pathogenesis and progression of PC are reported, and most of them are associated with androgen synthesis and androgen receptor (AR) signaling pathways.

The systemic cancer therapy includes chemotherapy, hormonal treatment and targeted biological therapies. However, these treatments are very costly and results in serious side effects, toxicity and drug resistance. Natural products serve as an arsenal of lead molecules and cause fewer undesirable side effects. The rhizomes of *Nelumbo nucifera* Gaetrn. (Nelumbonaceae) is a common vegetable cultivated in Asian countries for its medicinal and nutritive values. Pentacyclic triterpenoids are the major and bioactive phytoconstituents of *N. nucifera* rhizomes[7-10]. However, very few studies have been reported on *N. nucifera* triterpenoids.

The efficacy, bioavailability and pharmacokinetic properties of compounds can be optimized by structural modification by preparing their semi-synthetic analogues[11],for example naturally occurring triterpenoid oleanolic acid possess weak anticancer activity (*in vitro*) however its semi-synthetic derivative named bardoxolone (2-cyano-3,12-dioxooleana-1,9(11)-dien-28-oic acid; CDDO) has completed its phase 1 clinical trial to treat solid tumors and lymphomas serves a good example of lead optimization[12]. Identification of biological target is

the second important step followed by the lead optimization in drug discovery. Both ERα and AR are steroidal receptor family and play important role in the initiation and promotion of breast and prostate cancers[13]. In this study, ERα and AR were selected as receptors for docking studies. The aim of this study was therefore to investigate the antiproliferative activity of triterpenoids and their semi-synthetic derivatives, and establish the structure functional relationship.

Experimental section

General experimental procedures

All the solvents and reagents were LR grade. Silica-gels from SRL (India) were used for chromatographic separation. Melting points were uncorrected. IR spectra were recorded on FT-IR Perkin Elmer spectrum BX and $[\alpha]_D$ were measured on HORIBA, SEPA-300. NMR spectra were obtained on Bruker Avance Spectrometer (300 MHz for ^{1}H NMR and 75 MHz for ^{13}C NMR). Deuterated solvents for NMR were purchased from Sigma-Aldrich (USA).ESI-MS spectra were recorded on API 3000, Applied Biosystems, Canada. TLC of the compounds was determined on a pre-coated silica-gel 60 F254 plates (E MERCK, Darmstadt, Germany).

Semi-synthesis of triterpenoids

Methylation of triterpenoids **1**, **2** and **3**was carried out using diazomethane in diethyl ether at 0-5ºC to yield compounds **1a**, **2a** and **3a**. For acetylation, triterpenoids were dissolved in Ac_2O/pyridine at room temperature for 18 hrs. After usual workup and purification over silica-gel column chromatography acetyl derivatives 1b, 2b and 3c are yielded. The structures of compounds were confirmed by NMR, LC-MSand by comparing the spectral data with those reported in the literature. The chemical structures of triterpenoids are presented in Fig. 1.

In vitro antiproliferative activity

Testing of *in vitro* growth inhibition activity against human breast cell line MCF-7 (ATCC HTB 22) and prostate adenocarcinoma cell line PC-3 (ATCC CRL 1435) was performed by MTT assay[14] (Table 1). 2×10^3 cells/well were incubated in the 5% CO_2 incubator for 24 hr to enable them to adhere properly to the 96 well polystyrene micro plates (Grenier, Germany). Test compounds dissolved in 100% dimethyl sulphoxide (DMSO) were added at least in 5 doses and left for 6 hrs after which the compound plus media was replaced with fresh media and the cells were incubated for another 48 hr. in the

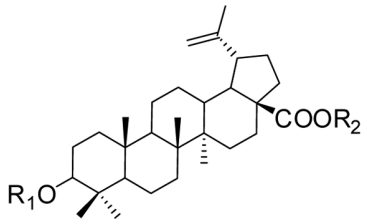

1 $R_1 = R_2 = H$; Betulinic acid
1a $R_1 = H$, $R_2 = CH_3$; Methyl betulinate
1b $R_1 = COCH_3$, $R_2 = H$; 3β-Acetoxy betulinic acid

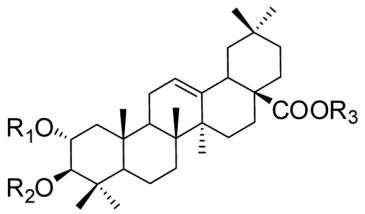

2 $R_1 = R_2 = R_3 = H$; Maslinic acid
2a $R_1 = R_2 = H$, $R_3 = CH_3$; Methyl maslinate
2c $R_1 = R_2 = COCH_3$, $R_3 = H$; 2α,3β-diacetoxy maslinic acid

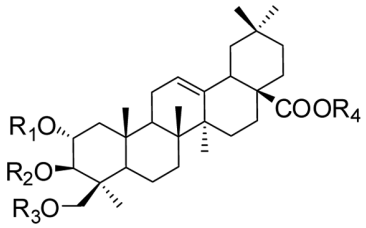

3 $R_1 = R_2 = R_3 = R_4 = H$; Hyptatic acid-A
3a $R_1 = R_2 = R_3 = H$, $R_4 = CH_3$; Hyptatic acid-A methyl ester
3b $R_1 = R_3 = COCH_3$, $R_2 = R_4 = H$; 2α,24-Diacetoxy hyptatic acid-A
3c $R_1 = R_2 = R_3 = COCH_3$, $R_4 = H$; 2α,3β,24-Triacetoxy hyptatic acid-A

Fig. 1 — Structures of triterpenoids and their derivatives.

CO_2 incubator at 37°C. The concentration of DMSO used in the experiments never exceeded 1.25%, which was found to be nontoxic to cells. Then, 10 µL MTT [3-(4, 5-dimethylthiazole-2-yl)-2,5-diphenyltetrazoliun bromide, Sigma M 2128] was added, and plates were incubated at 37°C for 4 hr. 100 µL DMSO was added to all wells and mixed thoroughly to dissolve the dark blue crystals. After few minutes at room temperature to ensure that all crystals were dissolved, the plates were read on a Spectra Max 190 Micro plate Elisa reader (Molecular devices Inc., USA) at 570 nm. Plates were normally read within 1 hr of adding the DMSO. The experiment was done in triplicate.

Molecular docking Simulation

The 3D docking analysis was carried out by AutoDockVina software using default parameters[15]. The structures of triterpenoids were drawn in ChemDraw Ultra 10.0 (CambridgeSoft Corporation, Cambridge, USA) and geometry optimization was performed through Avogadro software[16]. The crystal structures of ERα (PDB: 3ERT) and AR(PDB: 1E3G)proteins were retrieved from the protein data bank (www.rcsb.org/pdb). AutoDock tools was used to prepare the protein and ligands and saved in PDBQT format[17]. Autogrid program was used for the generation of grid parameters of 30 × 30 × 30 Åcube box from the center of co-crystallized ligands of ERα and AR. The Van der Waals and electrostatic terms were calculated by AutoDock parameter set and distance-dependent dielectric functions, respectively. The co-crystal ligands and water molecules were removed from proteins for docking purpose. The docking scores were denoted in terms of binding energy (BE) in kcal/mol. Graphical representations of the docking results were prepared using Discovery Studio 2017 R2 Client visualizer (Biovia).

The docking scores of antiproliferative active triterpenoids for ERα and AR are given in Table 2 and Table 3, respectively along with the hydrogen bonding and other interactions with amino acid residues of their respective enzymes. Docking analysis showed the high binding potential of compounds **3c** and **1** towards the active site of 3ERT with docking scores of –7.2 and –6.5 kcal/mol and their binding pose in the binding site of ERα are shown in Fig. 2a and 2b, respectively. The highest active compound **3c** formed one hydrogen bond interaction between one of the carbonyl oxygen (C=O) of the acetate group with –NH group of the CYS530. Compound **3c** showed one π–sigma stacking interaction and three π–alkyl interaction with TYR526 through one of the methyl group at ring E as well as three π–alkyl interactions with TYR526 in the binding pocket of ERα. The other key residues such as

Table 1 — Antiproliferative activity of triterpenoids and their derivatives.

Compd	IC_{50} (µM)	
	MCF-7	PC-3
1	17.54 ± 0.7	128.28 ± 5.2
1a	46.80 ± 2.5	IA
1b	IA	IA
2	55.08 ± 3.2	20.33 ± 1.0
2a	IA	102.88 ± 4.5
2b	81.0 ± 0.0	84.0 ± 0.0
3	77.86 ± 2.9	IA
3a	35.85 ± 2.1	19.52 ± 0.9
3b	69.93 ± 3.8	94.40 ± 4.4
3c	9.77 ± 0.9	60.26 ± 3.5
Doxorubicin	9.70 ± 0.5	9.20 ± 0.5

Tested concentrations: 1–200 µM; IA (inactive): IC_{50} > 200 µM.

Table 2 — Calculated binding energies (ΔG, kcal/mol) and interacting residues of receptor 3ERT.

Compd	MCF-7 (IC_{50} µM)	Docking Score (kcal/mol)	Interacting Residues
2α,3β,24-Triacetoxy hyptatic acid-A(**3c**)	9.77	–7.2	Asp351, Thr347, Ala350, Trp383, Met522, Tyr526, Leu536, Leu525, Lys529, Pro535, Val533, Met528
Betulinic acid (**1**)	17.54	–6.5	Tyr526, Cys530, Leu525, Met528, Thr347, Asp351, Ala350, Trp383, Val533, Leu536, Lys529, Pro535, Leu539, Leu354
Doxorubicin	9.7	–7.4	Asn519, Glu523, Met522, Leu525, Lys529, Cys530, Pro535, Tyr526, Leu536, Val533, Cys381, Glu380, Thr460, His377

Table 3 — Calculated binding energies (ΔG, kcal/mol) and interacting residues of receptor 1E3G.

Compd	PC-3IC_{50} (µM)	Binding Energy (kcal/mol)	Interacting Residues
Hyptatic acid-A methyl ester (**3a**)	19.52	–6.5	Tyr781, Ser782, Gln783, Glu872, Gln875, Lys883, Phe876, Asp879, Met780, His776, Arg779
Maslinic acid (**2**)	20.33	–6.3	Gln693, Asp690, His689, Ala699, Gly688, Ser703, Arg710, Ser703, Glu706, Asp809
Doxorubicin	9.2	–7.5	Glu678, Leu805, Phe804, Pro801, Trp751, Val684, Thr755, Asn756, Pro766, Tyr763, Arg752, Val685, Pro682, Gly683, Glu681, Ala748

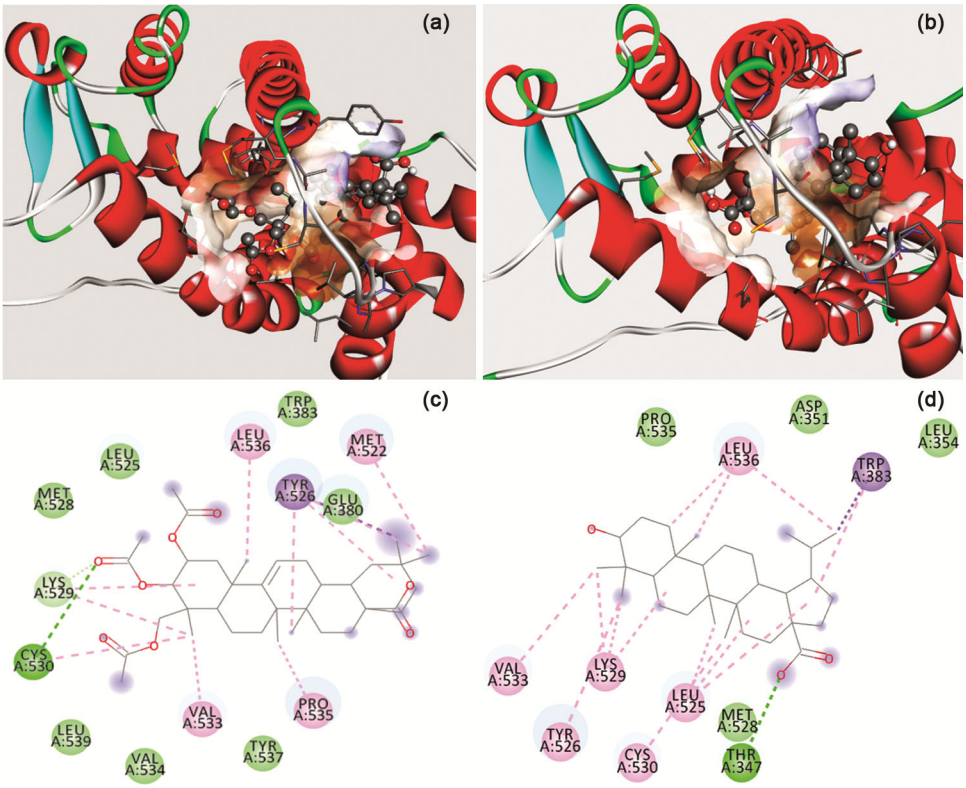

Fig. 2 — Molecular docking derived binding pose of **(a)** 2α,3β,24-Triacetoxy hyptatic acid-A and **(b)**betulinic acid within the active site of AR. The 2α,3β,24-triacetoxy hyptatic acid-A and betulinic acid shown as ball and stick model in the solid ribbon representation of the enzyme (Pdb id: 3ERT). The 2D interaction maps showing the molecular interactions of **(c)** 2α,3β,24-triacetoxy hyptatic acid-A and **(d)**betulinic acid with amino acids in AR active site.

MET528, Leu525, TRP383, GLU380, TYR537, VAL534, LEU539 and LYS529 were showingVan der Waals interactions, while LEU536, MET522, PRO535 and VAL533 have formed the alkyl interactions with compound **3c.** Similarly, docking simulations revealed that the top-scored docking pose (DS = –6.5 kcal/mol) of compound **1** (betulinic acid) showed a binding pattern similar to that of compound **3c**. However, the hydrogen-bonding pattern was slightly different from that of the compound **3c**. Compound **1** showed one hydrogen bond interaction between one the oxygen atom of carboxylic acid (COOH) group and –OH group of THR347.

In the active site of 1E3G, compounds **3a** and **2** showed docking scores of –6.5 and –6.3 kcal/mol and their binding pose in the binding site of AR are shown in Fig. 3a and 3b, respectively for prostate cancer. Compound **3a** showed π-alkyl interaction with ARG779 and three alkyl interactions with PHE876 against AR receptor. Amino acids TYR781, SER782, GLN783, GLU872, GLN875, LYS883, ASP879, MET780 and HIS776 showed Vander Waals interactions. In AR receptor, compound **2** showed one hydrogen bonding interaction between the hydrogen atom of carboxylic group (COOH) at C28 position with the oxygen atom of carboxylic group of ASP890. Compound **2** showed one π-alkyl interaction with HIS689 through angular methyl group at C10 position as well as three alkyl-alkyl interactions with ALA699 in the binding pocket of AR receptor.

Quantitative Structure Activity Relationship (QSAR) Modeling

In the present QSAR model, we included eight antiproliferative triterpenoids for MCF-7 and seven for PC-3 cells. The prediction ability of developed MCF-7 and PC-3 models were assessed on three triterpenoids as an external test (Fig. 1S) set reported by Bai *et al.* 2014[18]. The inhibitory activity of MCF-7 and PC-3 cell lines expressed as IC_{50} values in the micro-molar (μM) range were converted to the molar (M) range, and their negative logarithms (pIC_{50}) were used for the subsequent 2D-QSAR analysis as the response variable.

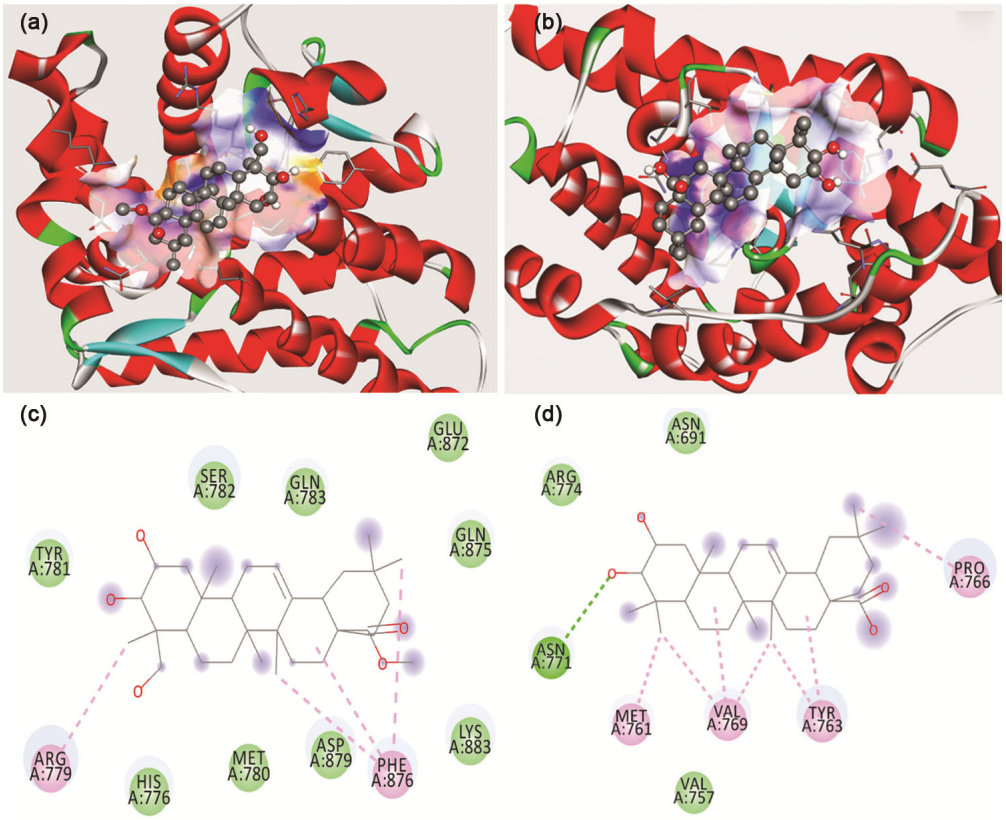

Fig. 3 — Molecular docking derived binding pose of **(a)** hyptatic acid-A methyl ester and **(b)** maslinic acid within the active site of AR. The hyptatic acid-A methyl ester and maslinic acid shown as ball and stick model in the solid ribbon representation of the enzyme (Pdb id: 1E3G).The2D interaction maps showing the molecular interactions of **(c)** hyptatic acid-A methyl ester and **(d)** maslinic acid with amino acids in AR active site.

pIC_{50}=– log (IC_{50})

The CDK (CDK v1.5.10) descriptors were used as independent variables to correlate the antiproliferative activity of triterpenoids with their structures[19]. Highly intercorrelated descriptors with a correlation index above 0.9 were removed. Furthermore, descriptors possessing zero standard deviation or a poor correlation with the dependent variable pIC_{50} were discarded. The most statistically significant descriptors were selected using the elimination selection-stepwise regression (ES-SWR) variable selection method. The selected descriptor set was then subjected to stepwise multiple linear regression (MLR) analysis to produce a linear model. The entire process of descriptor selection and model building was implemented in Weka using a *Meta* machine learning method called Attribute selected classifier[20]. Success of a QSAR model is to measure the quality off it on available training data set. The most common statistical qualities of equations were measured by the parameters such as explained variance (Ra^2), squared correlation coefficient (R^2), and mean absolute error (MAE)[21]. The robustness and predictivity of the models were evaluated by means of cross-validation, basically leave-two-out (L2O) were calculated with the training set and test set prediction[22]. The result from cross-validation procedure is cross-validated R^2_{L2O}, root mean square error (RMSE), and squared correlation coefficient of the test set (r^2), which are used as a criterion of both robustness and predictiveability of the QSAR models. Good quality of models is indicated by low MAE and low RMSE as well as by R^2, R^2_{L2O}values closed to one for training set, good prediction of test set and values of r^2 close to one.

Absorption, distribution, metabolism, excretion and toxicity studies

To ensure the drug likeness, all triterpenoids and doxorubicin were evaluated for their key physicochemical properties including predicted lipophilicity (log P), topological polar surface

area (TPSA), hydrogen bond donor (HBD), hydrogen bond acceptor (HBA) and number of rotatable bonds (nRotB) responsible for ADME as well as toxicity profile (AMES mutagenicity, tumorigenicity, reproductive effect and irritant) from OSIRIS Data Warrior Version 4.2.2 software[23].

Results and Discussion

Structure elucidation of triterpenoids

The structures of semi-synthetic derivatives (see Fig. 1) were confirmed by NMR and LC-MS analyses.

Compound 3a (Hyptatic acid-A methyl ester)

Colorless crystals, mp 126-128°C; $[\alpha]_D$ +28.75° (c 0.2, MeOH), IR (KBr) υ_{max} (cm^{-1}): 3422, 2947, 1727, 1654, 1458, 1161, 1051; ^1H NMR ($CDCl_3$, 300 MHz): 0.68 (3H, s), 0.84 (3H, s), 0.89 (3H, s), 0.92 (3H, s), 1.11 (3H, s), 1.21 (3H, s), 2.83 (1H, d, *J* = 11.4 Hz), 3.13 (1H, d, *J* = 9.3 H, H-3), 3.37 (1H, d, *J* = 10.5 Hz, H-24a), 3.83 (1H, m, H-2), 4.09 (1H, d, *J* = 10.8 Hz, H-24b), 5.27 (1H, s, H-12); ESI-MS: *m/z* 501.5 $[M-H]^+$ corresponding to $C_{31}H_{50}O_5$.

Compound 3b (2*α*,24-Diacetoxy hyptatic acid-A)

Colorless needles, mp 159°C; $[\alpha]_D$ +15.97°(c 0.2, MeOH); IR (KBr) υ_{max} (cm^{-1}): 3447, 2944, 1692, 1239, 1051;; ESI-MS: *m/z* 571.6 $[M-H]^+$.

Compound 3c (2*α*,3β,24-Triacetoxy hyptatic acid-A)

Colorless needles mp 147-152° C, $[\alpha]_D$ +23.98°(c 0.2, $CHCl_3$); IR (KBr) υ_{max} (cm^{-1}): 2946, 1743, 1631, 1459, 1371, 1240, 1044; ^1H NMR ($CDCl_3$, 300 MHz): δ 0.76 (s, Me), 0.91 (s, Me), 0.93 (s, Me), 1.03 (s, Me), 1.06 (s, Me), 1.12 (s, Me), 2.05 (s, 3 x Me), 2.84 (1H, d, *J* = 13.5 Hz, H-18), 4.20 (2H, br s, H-2 and H-3), 4.81 (1H, s, H-24a), 4.84 (1H, s, H-24b), 5.28 (1H, s, H-12). ESI-MS: *m/z* 637 $[M+Na]^+$ corresponding to molecular formula $C_{36}H_{54}O_8$.

In vitro antiproliferative activity

The triterpenoids were evaluated against MCF-7 and PC-3 cell lines for their antiproliferative activity and presented in Table 1. Amongst all compounds, **3c** (IC_{50} = 9.77 ± 0.9 μM) and **1** (IC_{50} = 17.54 ± 0.7 μM) showed strong antiproliferative activity against MCF-7 cells. While compound **3a** (IC_{50} = 19.52 ± 0.9 μM) and **2** (IC_{50} = 20.33 ± 1.0 μM) exhibited strong antiproliferative activity against PC-3 cells. Doxorubicin was used as a positive control with IC_{50} values 9.7 ± 0.5 μM and 9.2 ± 0.5 μM against MCF-7 and PC-3 cell lines, respectively.

Molecular Modeling

Computational docking of triterpenoids

Docking calculations for co-crystal compounds were carried out in ERα (PDB: 3ERT) and AR (PDB: 1E3G) to verify the docking protocol and reproduce the crystal structure geometry.Superimposition of the docked estradiol (PDB: 3ERT) and metribolone (PDB: 1E3G) onto their respective crystallographic geometry yielded the RMSD of 0.45 Å and 0.6 Å respectively, which confirms robustness of our docking protocol in reproducing experimentally observed binding conformations of both co-crystal compounds. This study confirmed its suitability for the present docking analysis. In this study, we have focused on the docking of two most active compounds **3c** and **1** in ERα for breast cancer, and compounds **3a** and **2** in AR for prostate cancer including standard drug doxorubicin to reveal the possible molecular determinants responsible for its binding affinities and biological activities (Tables 2 and 3).

QSAR Modeling

The computational strategies for QSAR, the most stable models obtained are presented in supplementary Table 1S and Fig. 1S, available at online**.** Using MLR method, we obtained the following best QSAR equations for MCF-7 and PC-3 cell lines derive for training dataset. For MCF-7 and PC-3 QSAR equation, two descriptors related to the anticancer activity of BC and PC was identified.

pIC_{50} (MCF-7) = 8.1274-0.2117*MOMI-XZ – 3.1006*geom. Shape

N = 8, R^2 = 0.96,R^2_a(adj.) = 0.9, S_{PRESS} = 0.135, MAE = 0.07, RMSE = 0.08, R^2_{L2O} = 0.83

N(test) = 3, r^2 (Test) = 0.87

pIC_{50} (PC-3) = 6.4842 –0.5553*ALogP – 0.0031*DPSA_1

N = 7, R^2 = 0.91,R^2_a(adj.) = 0.75, S_{PRESS} = 0.234, MAE = 0.12, RMSE = 0.12, R^2_{L2O} = 0.68

N(test) = 3, r^2 (Test) = 0.84

We obtained good models for both MCF-7 (R^2 = 0.96) and PC-3 (R^2 = 0.91) cell lines related to the BC and PC, respectively. The prediction of three external test set compounds from both MCF-7(r^2 = 0.87) and PC-3 (r^2 = 0.84) models are also quite predictive. Noting the sign of coefficients of each descriptor we observed that high values of MOMI-XZ and geom. Shape have a negative influence on the MCF-7 cell

inhibitory activity, as well as descriptors ALogP and DPSA_1 shows the negative effect on the inhibitory activity of triterpenoids for PC3 cell line. MOMI-XZ belongs to the moment of inertia (MI) descriptor class, characterizes the mass distribution and calculates the ratio of MI value along X and Z axis of molecules. The geom. Shape descriptor belongs to Petitjean shape indices class and based on molecular graph, which calculates the geometric shape index of the molecules. Hence, both descriptors suggest that low distributions of molecular mass as well as 3D shape of molecules are very important for MCF-7 inhibitory activity. ALogP descriptor depicts the molecular hydrophobicity (lipophilicity), usually quantified as (1-octanol/water partition coefficient) is an important molecular characteristic in drug discovery. DPSA_1 descriptor belongs to the Charged Partial Surface Area (CPSA) descriptors class and calculates the difference of partial positive surface area and partial negative surface area. So, the low hydrophobicity and optimum balance between the polar and non-polar groups are required for good PC3 inhibition, which is quite evident as all reported hyptatic acid-A derivatives have better PC3 inhibitory activity compare to hyptatic acid-A. So, we emphasized that in general the presence of more polar and less hydrophobic substituents makes these triterpenoids more effective inhibitors against both MCF-7 and PC3 cell lines.

Absorption, distribution, metabolism, excretion and toxicity (ADMET) studies

To ensure the drug likeness of triterpenoids and doxorubicin were used in the prediction of ADME/Toxicity tests and the results are presented in Table 4. In this study, we used our previously developed multiparameter optimization approach covering almost ~80% or more FDA approved anticancer drugs for eight important physicochemical properties ($200 < MW \leq 800$ Da, $1<$cLog P ≤ 5, $-6 \leq$ clog S ≤ -1, $5 \leq$ HBA ≤ 13, $1 \leq$ HBD ≤ 5, $50 \leq$ TPSA ≤ 180 Å^2, $0 \leq$ nRot ≤ 10, $1<$ log D ≤ 5) Singh, 2016[24]. The ADMET analysis for alltriterpenoids and doxorubicin were found to obey most of the physicochemical properties range with few exceptions as well as not showing any predicted toxicity. Doxorubicin is showing the deviation from logP, HDB and TPSA.

By establishing the correlation between *in vitro* results with *in silico* modeling and structure function attributes of triterpenoids, the key insights were derived as: (i) The increase in hydroxyl group (OH) from compounds **1** to **3** showed reduction in anticancer activity against MCF-7 cellline in a phased manner IC_{50} =17.54 ± 0.7 μM (**1**), 55.08 ± 3.2 μM (**2**) and 77.86 ± 2.9 μM (**3**). (ii) Hyptatic acid-A methyl ester **(3a)** exhibited higher activity in both MCF-7 (IC_{50} = 35.85 ± 2.1 μM) and PC-3 (IC_{50} = 19.52 ± 0.9 μM) cell lines compared to hyptatic acid-A, which can be partially attributed to the increase in the lipophilicity of **3a**and supported by the cLogP value (Table 4), as well as highest docking score and interaction within the AR. (iii) triacetyl derivative of hyptatic acid-A (**3c**) showed dramatically enhanced antiproliferative activity against MCF-7 cell line (IC_{50} = 9.77 ± 0.9 μM) possibly due to the increased lipophilicity and conformation preference of the molecule, which clearly seen through the high docking score and interactions of **3c** within the active site of ERα

Table 4 — Physicochemical properties of triterpenoids.

Compound	MW	cLogP	cLogS	HBA	HBD	Rotatable Bonds	Total Surface Area	Polar Surface Area	Mutagenic	Tumorigenic	Reproductive Effective	Irritant
1	456	6.37	–6.28	3	2	2	335	58	none	none	none	none
1a	470	6.80	–6.41	3	1	3	362	47	none	none	none	none
1b	498	6.86	–6.69	4	1	4	372	64	none	none	none	none
2	472	5.14	–5.62	4	3	2	336	78	none	none	none	none
2a	486	5.57	–5.75	4	2	3	349	67	none	none	none	none
2b	556	6.11	–6.44	6	1	6	394	90	none	none	none	none
3	488	4.29	–5.22	5	4	2	338	98	none	none	none	none
3a	502	4.71	–5.35	5	3	3	358	87	none	none	none	none
3b	572	5.25	–6.04	7	2	6	392	110	none	none	none	none
3c	614	5.74	–6.45	8	1	8	449	116	none	none	none	none
Doxorubicin	543	0.17	–4.51	12	6	5	398	206	none	none	none	high

(Fig. 2a). (iv) olean-12-ene skeleton, hyptatic acid-A derivatives (**3a**and **3c**) have better antiproliferative activity compared to maslinic acid derivatives (**2a**), suggesting the significant role of C-24 position (–OH and/or –$OCOCH_3$) for activity. (v) Interestingly, both betulinic acid and maslinic acid showed better activity compared to their derivatives, which is confirmed by their cLogP values, so the antiproliferative activity decreases if the cLogP value increases. These findings suggested further modification of triterpenoids against ERα and AR to develop new leads with better anticancer potential.

Conclusions

In this study, three new hyptatic acid-A derivatives **3a**, **3b** and **3c,** along with the first report of **1a** and **2b** for their antiproliferative activity against MCF-7 and PC-3 cell lines are reported. The molecular docking results of potent compounds provide a new insight about the possible pathway against BC and PC along with binding interactions in the active sites of ERα and AR. QSAR models of the triterpenoids were generated for MCF-7 and PC-3 cell lines showing good correlation coefficient with strong predictive ability of external test set compounds. QSAR model suggests the importance of geometrical shape and dipole moment of triterpenoids for the activity against MCF-7 cells, while AlogP and DPSA_1 is crucial for showing the activity against PC-3 cells. ADMET analysis demonstrated that the potent triterpenoids follow most of the physicochemical properties required for their optimum bioavailability and not showing any toxicity. The present study concluded that hyptatic acid-A is a good structural template to develop novel leads and substitution at C24-OH group has importance in bioactivity. Additionally, betulinic acid and maslinic acid have been used in food fortification to improve quality of life which signifies the nutritional value of *N. nucifera* rhizomes in dietary supplements and or/nutraceuticals for chemoprevention.

Supplementary Information

Supplementary information is available in the website http://nopr.niscpr.res.in/handle/123456789/58776.

References

1 Ferlay J, Ervik M, Lam F, Colombet M, Mery L, Piñeros M, Znaor A, Soerjomataram I & Bray F, *Global Cancer Observatory: Cancer Today. Lyon: International Agency for Research on Cancer* 2020, (https://gco.iarc.fr/today).
2 Anderson W F, Chatterjee, N, Ershler W B & Brawley O W, *Breast Can Res Treat*, 76 (2002) 27.
3 Suzuki K, Nakazato H, Matsui H, Koike H, Okugi H, Kashiwagi B, Nishii M, Ohtake N, Nakata S, Ito K &Yamanaka H, *Cancer,* 98 (2003) 1411.
4 Powles T J, *Nat Rev Can,* 2 (2002) 787.
5 Worldwide cancer data, World Cancer Research Fund International (wcrf.org), 2022.
6 Singh M, Jha R, Melamed J, Shapiro E, Hayward SW & Lee P, *Am J Pathol*, 184 (2014) 2598.
7 Chaudhuri P K & Singh D, *Nat Prod Res*, 27 (2013), 532.
8 Zhao X, Shen J, Chang K J & Kim S H, *J Agri Food Chem,* 62 (2014) 6227.
9 Hao C, Yu, Y, Zhang X, Dong G, Liu Y & Chen S, *J Food Qual*, 6 (2022) 1.
10 Yang H, He S, Feng Q, Liu Z, Xia S, Zhou Q, Wu Z & Zhang Y, *Biores Bioproc,* 11 (2024) 1.
11 Ren Y & Kinghorn D A, *Planta Med*, 85 (2019) 11.
12 http://clinicaltrials.gov
13 Valentín López J C, Lange C A & Dehm S M, *J Steroid Biochem Mol Biol*, 1 (2024) 106522.
14 Woerdenbag H J, Moskal T A, Pras N, Malingre T M, El-Feraly F S, Kampinga H H & Konings A W T, *J Nat Prod*, 6 (1993) 849.
15 Trott O & Olson A J, *J Comp Chem,*31 (2010) 455.
16 Hanwell M D, Curtis D E, Lonie D C, Vandermeersch T, Zurek E & Hutchinson G R, *J Cheminfo,* 4 (2012).
17 Morris G M, Huey R, Lindstrom W, Sanner M F, Belew R K, Goodsell D S & Olson A J, *J Comp Chem*, 30 (2009) 2785.
18 Bai L Y, Lin W Y, Weng J R, *Nat Prod Comm,* 9 (2014) 1557.
19 Steinbeck C, Hoppe C, Kuhn S, Guha R &Willighagen E L, *Curr Pharm Des*, 12 (2006) 2111.
20 Azuaje F, Witten I H & Frank E, *Bio Med Eng*, 5 (2006) 51.
21 Snedecor G W & Cochran W G, *Statistical Methods*, (Oxford & IBH Publishing, New Delhi), 1967, p381-418.
22 Kubinyi H, Hamprecht F A & Mietzner T, *J Med Chem*, 41 (1998) 2553.
23 Sander T, Freyss J, Korff M V & Rufener C, *J Chem Inf Mod*, 55 (2015) 460.
24 Singh D, *ADMET DMPK*, 4 (2016) 98.